

Influence of Preparation Conditions on the Self-Assembly by Stereocomplexation of Polylactide Containing Diblock Copolymers

D. Portinha, L. Bouteiller,* S. Pensec, and A. Richez

Laboratoire de Chimie des Polymères, UMR 7610 CNRS, Université Pierre et Marie Curie, tour 44, 1^{er} étage, 4 place Jussieu, 75252 Paris Cedex 05, France

C. Chassenieux

Physicochimie des Polymères et des Milieux Dispersés, UMR 7615 CNRS, Université Pierre et Marie Curie, ESPCI, 10 rue Vauquelin, 75231 Paris Cedex, France

Received December 4, 2003; Revised Manuscript Received February 20, 2004

ABSTRACT: Self-assembly of diblock copolymers having a crystallizable block can yield particles of complex shapes. Here, particles have been obtained by mixing two solutions of poly(L-lactide)–poly(ε-caprolactone) and poly(D-lactide)–poly(ε-caprolactone) diblock copolymers, in a good solvent of polycaprolactone. We have proved that these particles result from the cocrystallization of the polylactide blocks (stereocomplexation). At the highest concentration investigated (10 g/L), the stereocomplexation is in competition with a solvophobic driven aggregation process. However, the latter process is reversible and does not seem to affect the stereocomplexation to a large extent. At lower concentrations, stereocomplexation is the only process involved. Temperature also has a strong influence both on kinetics and on the structure of the particles. At low temperature, the growth of the particles is stopped at a particular size. This effect may be related to the properties of the polycaprolactone block.

Introduction

Self-assembly of AB block copolymers in a selective solvent of one of the blocks is often used to obtain well-defined nanoparticles that may have interesting properties for electronic, optical, or biomedical applications. In dilute solutions, when the insoluble A block forms amorphous aggregates, spherical micelles or vesicles are usually obtained. On the other hand, when the insoluble A block self-organizes within the aggregates, particles with a variety of shapes can result. This has been nicely demonstrated in the case of rod–coil block copolymers where the organization is driven by the packing of the rigid A blocks.¹ Organization within the core can also occur with flexible A blocks, if they crystallize. Such systems have been studied theoretically² and experimentally in the case of poly(ethylene oxide)–polystyrene^{3–5} and polyethylene–poly(ethylpropylene)⁶ diblock copolymers in hydrocarbon solvents. It was shown that these copolymers form thin platelet structures consisting of chain-folded crystalline domains of the insoluble block, surrounded by a solvated layer of the second block. The size of the particles can potentially be tuned by changing the length of each block, the solvent, or the temperature, but it is difficult to obtain stable dispersions of flat monodisperse nanoparticles of given lateral dimensions.

Here, our aim is to study the possibility to obtain nanoparticles in solution by cocrystallization of an AB and an A'B' diblock copolymer, such that the A and A' blocks can cocrystallize. The main advantage of such a system is that the molar ratio between the two diblocks can be used to potentially adjust the size of the nanoparticles. A second advantage is that particles can simply be obtained by mixing the solutions of each diblock. This preparative technique is soft and should make it possible to reach an equilibrium, which is not always granted with the usual techniques of cooling a warm solution or dialysis. Finally, the respective ordering of the A and A' blocks inside the cocrystal may

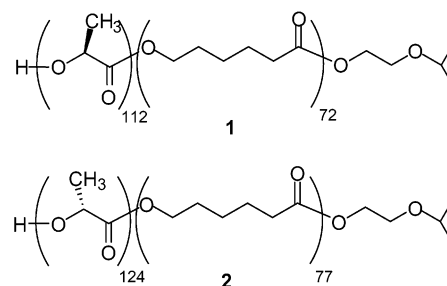


Figure 1. Structure of diblock copolymers **1** and **2**.

induce particular patterns in the corona (blocks B and B'), such as the formation of Janus particles.⁷

Poly(L-lactide) (PLLA) and poly(D-lactide) (PDLA) are semicrystalline polymers which form a racemic crystal (stereocomplex).⁸ The stereocomplex is much more stable than the crystals of each polyenantiomer because the chains are packed as pairs of helices of opposite configurations.⁹ Because of strong van der Waals interactions, the melting point of the stereocomplex is 50 °C higher than the melting point of both polyenantiomers. Thus, we synthesized poly(L-lactide)–poly(ε-caprolactone) (PLLA–PCL) **1** and poly(D-lactide)–poly(ε-caprolactone) (PDLA–PCL) **2** diblock copolymers (Figure 1) and studied their association in solution. We previously showed the feasibility of the concept in a preliminary report: particles are indeed obtained when solutions of **1** and **2** in tetrahydrofuran (THF) are mixed together.¹⁰ The aim of the present paper is to address the previously unanswered questions such as the following: (i) Are the particles obtained really due to the formation of the stereocomplex? (ii) What is the influence of preparation conditions on the formation of the particles?

Experimental Section

The synthesis and characterization of block copolymers **1** and **2** have been previously described.^{10,11}

Monitoring of the THF solutions of the copolymers by FTIR, ^1H NMR, and size exclusion chromatography revealed that no hydrolysis or degradation occurred within 1 year, if the solutions were kept in the dark, in carefully capped vials and at room temperature.

Dynamic light scattering measurements were performed with an experimental setup previously described,¹² at a wavelength (λ_0) of 514.5 nm. Samples were prepared by dissolving separately the same weight of each copolymer in THF (analytical reagent, Prolabo) at room temperature. Then, the solutions were filtered through Whatman Anotop filters (porosity 0.2 μm) and finally mixed together. The correlation functions were measured at the specified temperature and at various angles of observation (θ) ranging from 30° to 130° and have been analyzed thanks to the REPES routine.¹³ Depending on the mixtures, the distributions of relaxation times derived from the correlation functions were characterized by one or two relaxation processes. In all cases, the characteristic average relaxation times (τ) were q^2 -dependent, meaning that diffusive motions were probed. They could thus be used to calculate apparent diffusion coefficients $D = (q^2\tau)^{-1}$, where q is the scattering wave vector defined as $q = (4\pi n/\lambda_0 \sin(\theta/2))$ with n the refractive index of the solvent. Finally, an apparent hydrodynamic radius of the scattering species has been estimated using the Stokes–Einstein relation: $R_{h,\text{app}} = kT/6\pi\eta D$, where k is the Boltzmann constant, T the absolute temperature, and η the viscosity of the solvent.

Moreover, when the distributions of relaxation times were bimodal, a combination of the results from static and dynamic light scattering allowed to gain further quantitative information regarding the scattering species responsible for both relaxation processes, as established by Raspaud et al.¹⁴ This procedure is based on the fact that the total scattered intensity measured from static light scattering is a combination of the intensity scattered by the fast and the slow modes of relaxation obtained from dynamic light scattering. It will be shown later on that the fast relaxation process is due to the motion of free copolymer chains denoted unimers in the following, whereas the slow mode of relaxation is related to the motion of aggregates in solution. Thus, it can be written

$$I(q) = \frac{I_{\text{solution}}(q) - I_{\text{solvent}}(q)}{I_{\text{ref}}(q)} = I_{\text{uni}}(q) + I_{\text{agg}}(q) \quad (1)$$

where I_{solution} , I_{solvent} , and I_{ref} are the intensity scattered respectively by the solution, the solvent, and a reference (toluene).

In the same way, the correlation function is given by

$$g_1(q, t) = A_{\text{uni}}(q) \exp(-t/\tau_{\text{uni}}) + A_{\text{agg}}(q) \exp(-t/\tau_{\text{agg}}) \quad (2)$$

where $A_{\text{uni}}(q) + A_{\text{agg}}(q) = 1$. From both the concentration dependence of $I(q)$ and the amplitudes of each process of relaxation $A_{\text{uni}}(q)$ and $A_{\text{agg}}(q)$ extrapolated to zero angle, estimates of the free polymer chains concentration (C_{uni}) and of the apparent aggregation number (N_{agg}) may be obtained according to

$$C_{\text{uni}} = \frac{I_0 A_{\text{uni}}(q \rightarrow 0)}{KM_{\text{uni}}} \quad (3)$$

$$N_{\text{agg}} = \frac{M_{\text{agg}}}{M_{\text{uni}}} = \left(\frac{A_{\text{agg}}}{A_{\text{uni}}} \right)_{q \rightarrow 0} \frac{C_{\text{uni}}}{C - C_{\text{uni}}} \quad (4)$$

I_0 corresponds to the total scattered intensity extrapolated to zero angle. M_{uni} has been determined for freshly prepared solutions where initially no aggregation takes place. K is an optical constant defined as $K = (4\pi^2 n_{\text{ref}}^2 / R_{\text{ref}} \lambda_0^4 N_a) (dn/dC)^2$, where $n_{\text{ref}} = 1.496$ and $R_{\text{ref}} = 0.33 \times 10^{-4} \text{ cm}^{-1}$ are respectively the refractive index and the Rayleigh ratio of toluene. N_a is the Avogadro constant, and dn/dC is the specific refractive index increment, which has been measured for **1** by differential refractometry ($dn/dC = 0.061 \text{ mL/g}$). Last, thanks to the small

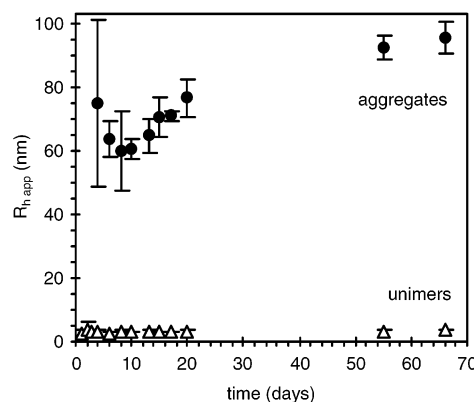


Figure 2. Apparent hydrodynamic radii for a 10 g/L solution of **1** in THF vs time after dissolution ($T = 25^\circ\text{C}$).

size of the unimers, the q dependence of $I(q)$ is driven by the contribution of the apparent radius of gyration for the aggregates ($R_{g,\text{agg}}$) according to

$$\frac{1}{I(q)} = \frac{1}{I_0} \left(\frac{1 + q^2 R_{g,\text{agg}}^2}{3} \right) \quad (5)$$

Two main assumptions are made when using this procedure: the first one is the neglect of the interactions between unimers and/or aggregates, and the second one is that the contrast of aggregates in solution is supposed to be the same as the contrast of unimers.

Infrared spectra were recorded at room temperature on a Nicolet Avatar 320 FTIR spectrometer in KBr cells of 0.015–0.1 cm path length. The spectra were corrected by subtracting the spectrum of pure THF in the same cell. Stereocomplex conversion was deduced from the intensity of the $\nu_{\text{C=O}}$ lactide vibration band (1763 cm^{-1}) after fitting the experimental spectra between 1700 and 1800 cm^{-1} to a combination of three Lorentzian curves.

Differential scanning calorimetry was performed with a TA Instrument 2920 modulated DSC.

Results and Discussion

Before focusing on the self-assembly of the mixture of copolymers **1** and **2**, the behavior of each copolymer alone is described.

1. Behavior of the Reference: Copolymer 1 Alone. Diblock copolymer **1** was easily dissolved in THF at room temperature to obtain a clear solution at a concentration of 10 g/L. However, dynamic light scattering revealed that some aggregation occurred because a bimodal distribution of the relaxation times was obtained.¹⁰ Figure 2 shows that the hydrodynamic radius of the fast component remains constant over time ($R_{h,\text{app}} = 3 \pm 0.5 \text{ nm}$). This fast component corresponds to individual diblock copolymer chains. The hydrodynamic radius of the slow component, however, increases up to 90 nm within 2 months. To evaluate the concentration of aggregates and their aggregation number, the combined dynamic and static light scattering data were analyzed according to Raspaud et al., as detailed in the experimental procedure.¹⁴

The concentrations of free chains and aggregates are approximately constant over 2 months (Figure 3), but the size of the aggregates increases steadily (Figures 2 and 4). This behavior can possibly be explained by a two-step mechanism. First, the amphiphilic nature of the copolymer is responsible for the formation of particles in equilibrium with free copolymer chains. The concentration of free chains remains constant and equal to 8

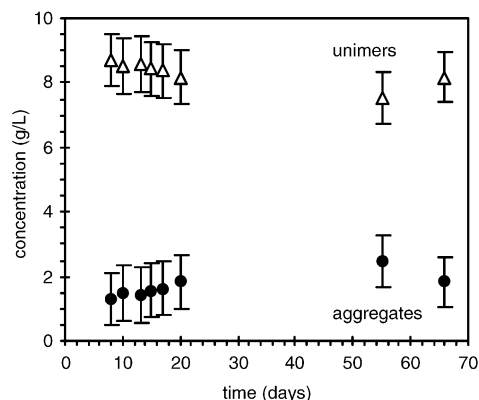


Figure 3. Concentrations of free chains and aggregates for a 10 g/L solution of **1** in THF vs time after dissolution ($T = 25\text{ }^{\circ}\text{C}$).

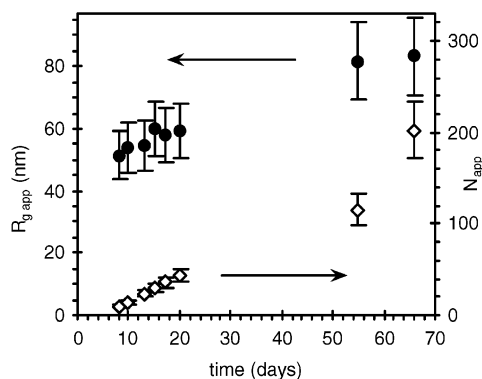


Figure 4. Apparent radius of gyration and aggregation number for the aggregates in a 10 g/L solution of **1** in THF vs time after dissolution ($T = 25\text{ }^{\circ}\text{C}$).

g/L, whatever the aging of the solution. This phenomenon could be due to the poor affinity of the PLLA block for THF and is equivalent to the micellization of an amphiphilic diblock copolymer in water.¹⁵ Then, these particles have a tendency to self-associate. The size of the formed aggregates grows with time, but this second aggregation does not affect the overall concentration of free chains.

An important question is to know what is the physical state of the PLLA chains in the core of the micelles. Monitoring the solutions with ^1H NMR spectroscopy revealed no evolution of the spectra over more than 5 months. It means that the PLLA chains retain some mobility within the aggregates and are not crystallized.

2. Mixture of Copolymers 1 and 2. Fresh solutions of **1** and **2** at 10 g/L in THF were prepared separately and mixed together. Static light scattering (Figure 5) and dynamic light scattering¹⁰ show that particles are formed more rapidly and are larger than the aggregates previously detected in solutions of the single copolymer **1** or **2**. Moreover, as noted before,¹⁰ the size distribution of the aggregates is much narrower in the case of the mixture of **1** and **2** than in the case of the single copolymer.

After 8 days, the solution turned cloudy, and after 1 month, a thin precipitate formed. FTIR spectroscopy (Figure 6) unambiguously proves that the formation of the stereocomplex is the driving force of this self-assembly. Indeed, the carbonyl vibration band characteristic of disordered polylactide chains (at 1763 cm^{-1}) gradually disappeared, and a new vibration band (at 1747 cm^{-1}) appeared. This vibration has previously been

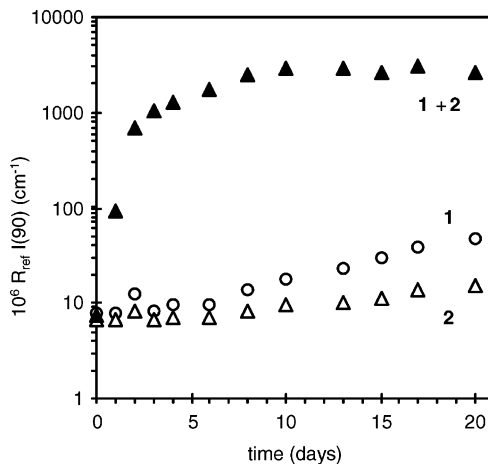


Figure 5. Time dependence of the scattered intensity measured at $\theta = 90^{\circ}$ for solutions of **1**, **2**, and their mixture ($C = 10\text{ g/L}$, $T = 25\text{ }^{\circ}\text{C}$).

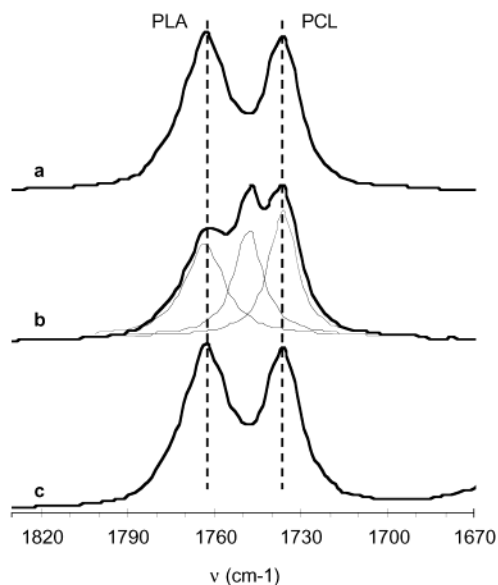


Figure 6. FTIR spectra of a solution in THF containing **1** and **2**, immediately after mixing (a) and 48 days after mixing (b). Reference spectrum of a solution of **1** in THF, 48 days after dissolution (c) ($C = 10\text{ g/L}$, $T = 25\text{ }^{\circ}\text{C}$).

attributed to the polylactide chains involved in the stereocomplex, which are in a 3_1 helix conformation.¹⁶

After deconvolution of the signal, it is possible to monitor the decrease of the band at 1763 cm^{-1} and thus to measure the conversion of the stereocomplexation. The conversion determined by FTIR is compared in Figure 7 with the conversion previously measured by ^1H NMR spectroscopy,¹⁰ from the decrease of the intensity of the signal at 5.28 ppm, corresponding to the polylactide methine group. Of course, the two techniques do not reveal exactly the same phenomenon because the FTIR analysis measures the number of chains in a 3_1 helix conformation and the ^1H NMR analysis is sensitive to the number of chains that are still mobile. However, this should not make a large difference, and the agreement between the two techniques is gratifying.

These curves show that the formation of the stereocomplex is not monotonic: a relatively fast growth is followed by a slower increase after 30 days. This slowdown is possibly due to the fact the particles started to settle down after 1 month.

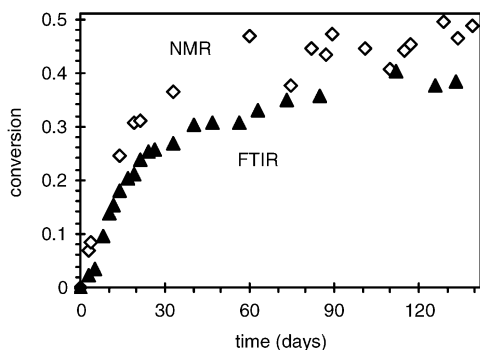


Figure 7. Time dependence of the conversion measured by FTIR or ^1H NMR for a solution of **1** and **2** ($C = 10$ g/L, $T = 25$ °C).

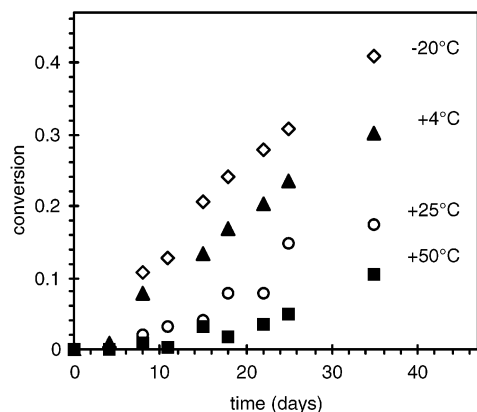


Figure 8. Time dependence of the conversion measured by FTIR for solutions of **1** and **2** at different temperatures ($C = 3$ g/L).

The most important conclusion derived from Figure 7 is that the conversion is far from quantitative: after 2 months, roughly one-third of the polylactide is involved in the particles. This is not in contradiction with the fact that no free chains were detected after 1 day by dynamic light scattering.¹⁰ Indeed, the particles are so large that their contribution to the scattering is overwhelming.

Next, the influence of different parameters on the formation of the stereocomplex was investigated.

2.1. Influence of Temperature. Solutions of **1** and **2** at 3 g/L in THF were prepared and immediately mixed together. This solution was then split in four, and each solution was stored at a different temperature between -20 and $+50$ °C. Figure 8 shows that the lower the temperature, the faster is the formation of the stereocomplex. This behavior is consistent with the fact that stereocomplexation is a crystallization process: at a lower temperature, the degree of undercooling is larger, and thus the driving force for stereocomplexation is increased.

The effect of temperature on the size of the particles (Figure 9) is not so straightforward, in part because the measured hydrodynamic radius is an apparent value, which depends on concentration through the dynamic second virial coefficient (k_d): $R_{h,app} = R_{h0}/(1 + k_d C)$, with R_{h0} the value for the hydrodynamic radius extrapolated to zero concentration. Not only is the temperature dependence of k_d unknown, but the value of k_d might also change with time (with the molar mass and the structure of the aggregates). Nevertheless, the apparent hydrodynamic radii for the particles formed at 50 °C are smaller than those obtained at 25 °C, which is in

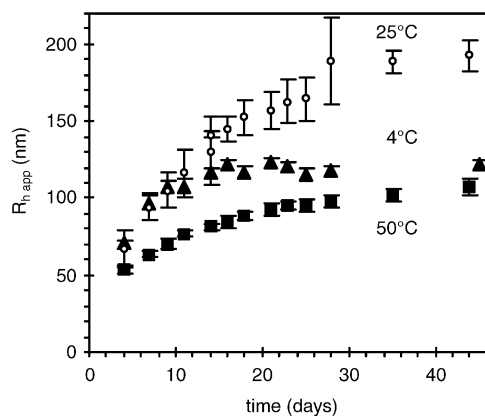


Figure 9. Time dependence of the apparent hydrodynamic radius of the particles formed in solutions of **1** and **2** at different temperatures ($C = 3$ g/L).

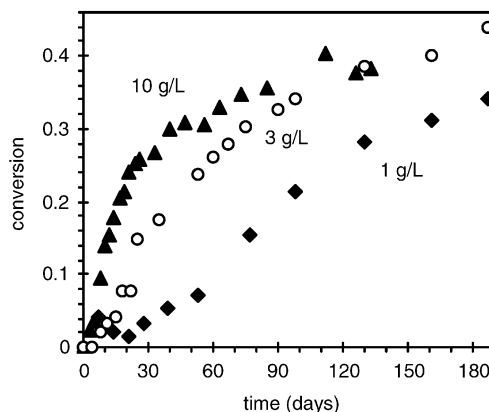


Figure 10. Time dependence of the conversion measured by FTIR for solutions of **1** and **2** at different concentrations ($T = 25$ °C).

agreement with the slower growth due to undercooling. On the other hand, at 4 °C the particles first grow at the same rate as at 25 °C, and then after 20 days, the growth of the particles seems to be stopped. This behavior at 4 °C is very intriguing because it implies that a process which limits the size of the particles at about 120 nm is at work. It is possible that this process is related to the coil–globule transition of PCL, which is known to occur at about 0 °C.¹⁷ Indeed, a more compact conformation of the PCL block could be responsible for the formation of a denser shell around the particles, which could stop the growth at some point.

The exact nature of this process remains to be proved, but it would be very useful to be able to tune it to tailor-make the structure of the particles.

2.2. Influence of Concentration. Fresh solutions of **1** and **2** at 1, 3, or 10 g/L in THF were prepared separately and combined. As previously mentioned, the mixture at 10 g/L turned cloudy after 8 days and finally precipitated, but the mixtures at 1 and 3 g/L remained perfectly clear for several months. Figure 10 shows that the stereocomplex is still steadily formed in the solutions at 1 and 3 g/L, 6 months after their preparation. This confirms the fact that the slowdown of the growth for the 10 g/L solution is connected to the precipitation of the particles. Moreover, Figures 10 and 11a show that the lower the concentration of the solution, the slower are the conversion and the growth of the particles. Apart from this expected kinetic effect, it is interesting to compare the size of particles in the different solutions when the same quantity of stereocomplex is formed.

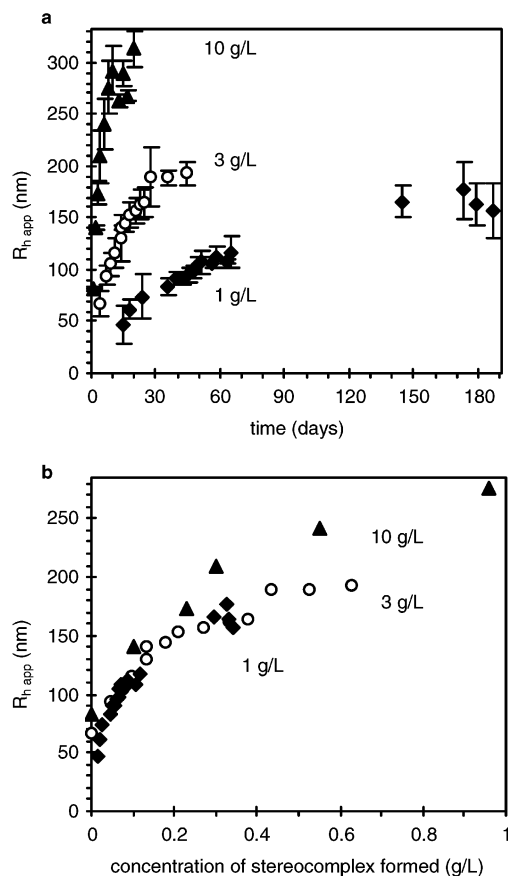


Figure 11. Apparent hydrodynamic radius of the particles formed in solutions of **1** and **2** at different concentrations vs time (a) or vs the concentration of stereocomplex formed (b) ($T = 25\text{ }^{\circ}\text{C}$).

Figure 11b shows that for low quantities of stereocomplex the apparent hydrodynamic radius of the particles does not depend on the concentration of the starting solution. Consequently, at low conversions, the structure of the particles is probably independent of the concentration of the starting solution, and the concentration dependence of the apparent hydrodynamic radius (k_d) is constant or the same. This is no more the case for concentrations of stereocomplex higher than 0.2 g/L: the particles in the 10 g/L solution are larger than the particles in the 1 or 3 g/L solutions. The larger size of the particles obtained at 10 g/L is in agreement with the precipitation observed after 1 month.

It is to be noted that, whatever the concentration, the polydispersity of the aggregates does not increase noticeably with time. It means that if new aggregates are formed continuously, they do not contribute significantly to the scattered intensity.

2.3. Influence of the Maturation of the Mother Solutions. In the case of solutions at 10 g/L, we have shown that each copolymer alone slowly forms aggregates. It is thus interesting to see whether the formation of the particles by stereocomplexation is influenced by the age of the mother solutions. Consequently, a solution of **1** and **2** at 10 g/L prepared in the usual way was compared to a solution of identical composition but obtained by mixing a solution of **1** and a solution of **2** which had been prepared 56 days before. For convenience, we will call these solutions respectively “fresh” or “matured”.

Concerning the matured solution, three main behaviors could be encountered if it is compared to a fresh

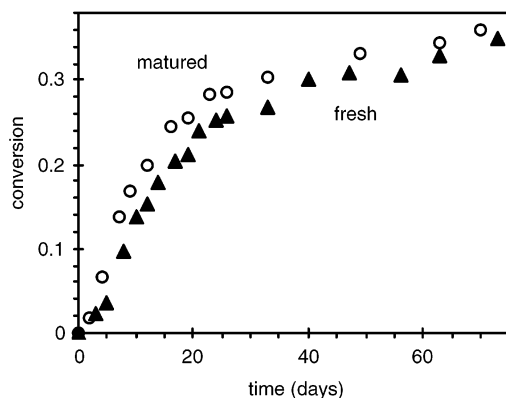


Figure 12. Time dependence of the conversion measured by FTIR for fresh or matured solutions of **1** and **2** ($C = 10\text{ g/L}$, $T = 25\text{ }^{\circ}\text{C}$).

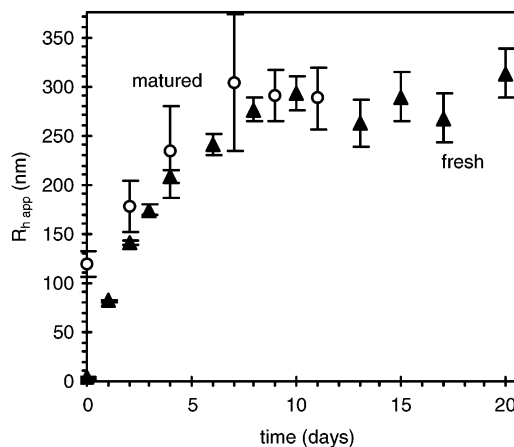


Figure 13. Time dependence of the apparent hydrodynamic radius of the particles formed in fresh or matured solutions of **1** and **2** ($C = 10\text{ g/L}$, $T = 25\text{ }^{\circ}\text{C}$).

solution of the same age after mixing **1** and **2**: (a) If the aggregates of **1** and **2** are not involved in the formation of the stereocomplex, then the conversion and the size of the stereocomplex particles should be lower for the matured solution because fewer free chains are available for the stereocomplexation. (b) If the aggregates of **1** and **2** are incorporated without reshuffling in the stereocomplex particles, then the conversion in stereocomplex of the matured solution should be lower than or equal to the conversion of the fresh solution, but the size of the stereocomplex particles should be larger for the matured solution. (c) If the aggregates of **1** and **2** are incorporated and converted into the stereocomplex, then both the conversion and the size of the stereocomplex particles should be larger for the matured solution.

Figures 12 and 13 show that the influence of maturation on the formation of the stereocomplex particles is not very strong. However, the conversion in stereocomplex and the size of the particles are significantly larger for the matured solution. This is in agreement with mechanism c, which means that the aggregates of **1** and **2** may be incorporated in the particles and that the chains of polylactide in these aggregates may be sufficiently mobile to diffuse until they cocrystallize.

To confirm this hypothesis, different solutions were evaporated as fast as possible under vacuum and then analyzed by DSC. Figure 14a shows the first heating scan of a sample obtained by evaporation of a solution of **1** and **2**, just after mixing the fresh mother solutions.

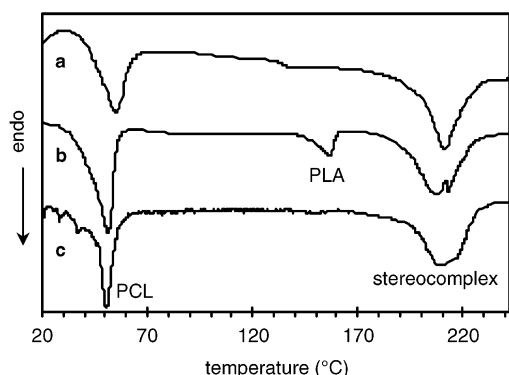


Figure 14. First DSC heating scan of evaporated solutions of **1** and **2** in THF (10 g/L). Fresh solution evaporated just after mixing (a), solutions matured for 58 days, mixed, and evaporated 2 days later (b), solutions matured for 58 days, mixed, and evaporated 18 days later (c).

The thermogram shows only an endotherm corresponding to the melting of the stereocomplex (beside the melting of PCL). Since the stereocomplex had no time to form in solution, it means that it was formed quantitatively during the evaporation. It is well-known that the stereocomplex is easily formed by evaporation.¹⁸ Figure 14b shows the first heating scan of a sample obtained from a matured solution of **1** and **2** and evaporated 2 days after mixing the mother solutions. In this case, an additional endotherm corresponding to polylactide melting is detected: it confirms the presence of aggregates of pure **1** and pure **2**, 2 days after mixing the matured mother solutions. Finally, Figure 14c shows the first heating scan of a sample obtained from the same matured solution but evaporated 18 days after mixing the mother solutions. No more melting of polylactide is detected: it confirms that the aggregates of pure **1** and pure **2** have reorganized to form the stereocomplex within 18 days.

Conclusion

It is possible to form particles simply by mixing two solutions of diblock copolymers containing complementary blocks of PLLA and PDLA. We have proved that these particles result from the cocrystallization of the polylactide blocks (stereocomplexation). At the highest concentration investigated (10 g/L), the stereocomplexation is in competition with a solvophobic driven aggregation process. However, the latter process is reversible and does not seem to affect the stereocomplexation to a large extent. At lower concentrations, stereocomplexation is the only process involved. Temperature also has a strong influence both on kinetics

and on the structure of the particles. At low temperature, the growth of the particles seems to be stopped at a particular size. It is possible that this effect is related to the properties of the polycaprolactone block. The shape of the particles obtained by the present scheme is currently under study.

Acknowledgment. Purac Co. is acknowledged for providing the lactide monomers used in this work.

References and Notes

- (1) (a) Lee, M.; Cho, B.-K.; Zin, W.-C. *Chem. Rev.* **2001**, *101*, 3869. (b) Klok, H.-A.; Lecommandoux, S. *Adv. Mater.* **2001**, *13*, 1217.
- (2) (a) Birshtein, T. M.; Zhulina, E. B. *Polymer* **1990**, *31*, 1312. (b) Vilgis, T.; Halperin, A. *Macromolecules* **1991**, *24*, 2090.
- (3) (a) Lotz, B.; Kovacs, A. J. *Kolloid Z. Z. Polym.* **1966**, *209*, 97. (b) Lotz, B.; Kovacs, A. J.; Bassett, G. A.; Keller, A. *Kolloid Z. Z. Polym.* **1966**, *209*, 115.
- (4) (a) Cogan, K. A.; Gast, A. P. *Macromolecules* **1990**, *23*, 745. (b) Gast, A. P.; Vinson, P. K.; Cogan-Farinas, K. A. *Macromolecules* **1993**, *26*, 1774. (c) Lin, E. K.; Gast, A. P. *Macromolecules* **1996**, *29*, 4432.
- (5) Reiter, G.; Hoerner, P.; Hurtrez, G.; Riess, G.; Sommer, J.-U.; Joanny, J.-F. *J. Surf. Sci. Technol.* **1998**, *14*, 93.
- (6) (a) Richter, D.; Schneiders, D.; Monkenbusch, M.; Willner, L.; Fetters, L. J.; Huang, J. S.; Lin, M.; Mortensen, K.; Farago, B. *Macromolecules* **1997**, *30*, 1053. (b) Monkenbusch, M.; Schneiders, D.; Richter, D.; Willner, L.; Leube, W.; Fetters, L. J.; Huang, J. S.; Lin, M. *Physica B* **2000**, *276–278*, 941.
- (7) Erhardt, R.; Böker, A.; Zettl, H.; Kaya, H.; Pyckhout-Hintzen, W.; Krausch, G.; Abetz, V.; Müller, A. H. E. *Macromolecules* **2001**, *34*, 1069.
- (8) Ikada, Y.; Jamshidi, K.; Tsuji, H.; Hyon, S.-H. *Macromolecules* **1987**, *20*, 904.
- (9) (a) Okihara, T.; Tsuji, M.; Kawaguchi, A.; Katayama, K. *J. Macromol. Sci., Phys.* **1991**, *30*, 119. (b) Brizzolara, D.; Cantow, H.-J.; Diederichs, K.; Keller, E.; Domb, A. J. *Macromolecules* **1996**, *29*, 191. (c) Cartier, L.; Okihara, T.; Lotz, B. *Macromolecules* **1997**, *30*, 6313.
- (10) Portinha, D.; Belleney, J.; Bouteiller, L.; Pensec, S.; Spassky, N.; Chassenieux, C. *Macromolecules* **2002**, *35*, 1484.
- (11) Simic, V.; Pensec, S.; Spassky, N. *Macromol. Symp.* **2000**, *153*, 109.
- (12) Chassenieux, C.; Nicolai, T.; Durand, D. *Macromolecules* **1997**, *30*, 4952.
- (13) Stepanek, P. In *Dynamic Light Scattering: The Method and Some Applications*; Brown, W., Ed.; Clarendon Press: Oxford, 1993; Chapter 4.
- (14) Raspaud, E.; Lairez, D.; Adam, M.; Carton, J.-P. *Macromolecules* **1994**, *27*, 2956.
- (15) The existence of this critical concentration is confirmed by the fact that no aggregation is observed for solutions of **1** at a concentration of 1 or 3 g/L.
- (16) Kister, G.; Cassanas, G.; Vert, M. *Polymer* **1998**, *39*, 267.
- (17) Piçarra, S.; Gomes, P. T.; Martinho, J. M. G. *Macromolecules* **2000**, *33*, 3947.
- (18) Tsuji, H.; Hyon, S.-H.; Ikada, Y. *Macromolecules* **1991**, *24*, 5651.

MA035831E